

# Comparison of fluid and particle-in-cell simulations on atmospheric pressure helium microdischarges

Y J Hong<sup>1,2</sup>, M Yoon<sup>2</sup>, F Iza<sup>3</sup>, G C Kim<sup>4</sup> and J K Lee<sup>1,5</sup>

<sup>1</sup> Department of Electronic and Electrical Engineering, Pohang University of Science and Technology, Pohang 790-784, Korea

<sup>2</sup> Department of Physics, Pohang University of Science and Technology, Pohang 790-784, Republic of Korea

<sup>3</sup> Department of Electronic and Electrical Engineering, Loughborough University, Loughborough, Leicestershire LE11 3TU, UK

<sup>4</sup> Department of Oral Anatomy, College of Dentistry, Pusan National University, Busan 602-739, Republic of Korea

E-mail: [jk1@postech.ac.kr](mailto:jk1@postech.ac.kr)

Received 17 September 2008, in final form 15 October 2008

Published 27 November 2008

Online at [stacks.iop.org/JPhysD/41/245208](http://stacks.iop.org/JPhysD/41/245208)

## Abstract

Microdischarges at atmospheric pressure were studied by two computational methods. The first method is a typical one-dimensional fluid model in which the electron velocity distribution function is assumed to be Maxwellian and the energy equation is solved to determine the spatial profile of the electron temperature. The second method is a particle-in-cell (PIC) model with Monte-Carlo collisions (MCC). We compared the time-averaged density, electric field and power consumption profiles of helium microdischarges driven at 13.56 MHz and 2.45 GHz obtained with the two models. The agreement between the two models depends on the driving frequency. The kinetic information obtained from the PIC-MCC model indicates that the improved agreement at higher frequency is due to the evolution of the electron energy distribution function from a three-temperature distribution at 13.56 MHz to a close-to-Maxwellian distribution at 2.45 GHz.

(Some figures in this article are in colour only in the electronic version)

## 1. Introduction

Microdischarges at atmospheric pressure have been studied for use in novel biomedical applications [1–3]. With small dimensions ranging from tens of micrometres up to a few millimetres, experimental characterization of these discharges is very challenging. Probe techniques used to study particle kinetics in large scale low-pressure discharges [4] turn impractical as the dimensions of the plasma reduce. Moreover, there is a lack of an appropriate theory to interpret the data measured in atmospheric pressure discharges. Optical diagnostics are typically preferred since they offer a non-invasive means to study these microdischarges. Space- and

time-resolved measurements of microdischarges, however, demand complex experimental setups [5, 6] and require involved theoretical models to account for the collisional processes that dominate atmospheric pressure discharges. Although laser-aided diagnostics and mass spectrometry have also been used to study these devices, they also face challenges due to the high collisionality and small dimensions of atmospheric pressure microdischarges. Given these experimental challenges, computer simulations provide an alternative method of analysing high-pressure microplasmas, contributing to the advance in our current understanding of the underlying physics. Fluid (or hydrodynamic), particle-in-cell (PIC) and hybrid methods can be used to simulate low-temperature plasmas [7–11]. In this study we focused on the first two methods and compared the results obtained

<sup>5</sup> Author to whom any correspondence should be addressed.

when modelling a plasma needle. Through the comparison, it was found that a better agreement between the fluid and PIC simulation models was obtained at high frequency. In the dc (zero frequency) discharges, fluid simulations could not describe the features observed in particle-in-cell Monte-Carlo collision (PIC-MCC) simulations [10].

Fluid models solve a set of moments of the Boltzmann equation for each species in the plasma. In this work the first three moments are considered, which result in the continuity, momentum and energy balance equations [9]. Because in atmospheric pressure plasmas the momentum-transfer-collision frequency is much larger than the RF or microwave driving frequency, the drift-diffusion approximation is typically used [9]. This approximation eliminates the momentum-balance equation and reduces the overall computational cost of the model. The above mentioned equations are solved with Poisson's equation in order to account for the self-consistent electric field. In order to facilitate a fair comparison between the simulation results of the fluid and PIC-MCC models, the reactions considered in the two models are the same. Ions and electrons are created by electron-impact ionization of ground state atoms and the ionization rate is expressed as a function of the electron temperature. The electron temperature is obtained as a solution of the electron energy balance equation, which accounts for energy losses due to elastic and inelastic (excitation and ionization) collisions. The transport coefficients (e.g. the mobility and the diffusion constants) and the collisional frequencies (e.g. ionization and momentum transfer collisional frequencies) are pre-computed as a function of the mean electron energy assuming that the electron velocity (energy) distribution function is Maxwellian. Solving the set of fluid equations yields the plasma density, potential and electron energy profiles that are presented here.

The PIC-MCC model used in this work has been extensively used in the study of low-temperature plasmas [12, 13] and only the most important features of this model are highlighted here. PIC simulations take advantage of the collective behaviour of charged particles in plasmas and model the kinetics of various species by simulating a reduced number of particles. Collisions are incorporated in the simulation by applying an MCC scheme that statistically determines the particles undergoing collision and their scattered velocities. For electrons, elastic, excitation and ionization collisions are considered in the model. For ions, charge exchange and elastic scattering collisions are modelled. Reactions of excited atoms and Coulomb collisions are not considered in this study. Note that the same set of reactions is considered in the fluid and PIC-MCC model in order to facilitate a fair comparison between the results obtained with the two models. At the boundaries the interaction between particles and the electrodes is modelled accounting for secondary electron emissions and the boundary conditions imposed by the external electrical circuit.

## 2. Simulation conditions

One-dimensional fluid and PIC-MCC models were used to model needle discharges sustained at RF and microwave

frequency. The plasmas were sustained in helium at the atmospheric pressure (760 Torr). The asymmetry of the discharge due to the different areas of the ground electrode and the powered needle is captured in the one-dimensional model using a coaxial configuration. The inner electrode representing the needle has a radius of 0.03 mm and is powered by either a current or voltage source. The gap between the inner and the outer electrodes is set to 200  $\mu\text{m}$  and the outer electrode is grounded. The RF (13.56 MHz) power source was set to an rms value of 1.6 A  $\text{cm}^{-2}$ . For the microwave case (2.45 GHz), the current source was varied from 7.4 to 15 rms A  $\text{cm}^{-2}$  and the voltage source between 90 and 135 V. For the stability and accuracy of the simulations, restrictions on some numerical parameters such as the cell size and time step need to be considered [9, 12]. In our simulations, we used 200 cells (1  $\mu\text{m}$  spatial resolution) and a time step of  $(1-5) \times 10^{-14}$  s. In order to reduce the statistical noise due to the limited number of super-particles in the PIC simulation, a digital smoothing algorithm was applied to the space charge [12]. The helium gas was assumed to remain at room temperature and gas flow was not considered in the simulations. The ground state helium atoms were assumed to be distributed uniformly over the discharge space and traces of molecular gases often encountered in open-air discharges had been neglected in this study.

## 3. Results and discussion

An earlier work reported on the similarities and differences between the results obtained with fluid and PIC codes when simulating RF discharges [14]. In that work helium atmospheric pressure RF discharges driven at different current levels were studied. It was found that a better agreement between the two simulation models was obtained at low current. In this work we compare the results of the two simulation codes as a function of the driving frequency. The density, electric field and power deposition profiles of helium atmospheric pressure discharges driven at 2.45 GHz and 13.56 MHz are shown in figures 1 and 2, respectively. The profiles are time averaged over an excitation cycle. Figure 1(a) indicates that the predictions made with the two models at 2.45 GHz are quite in agreement. As the frequency decreases, however, the discrepancy increases and the PIC-MCC model for RF discharge predicts a much larger density than the fluid model (figure 2(a)). The same tendency is observed in the power deposition profiles where the agreement between fluid and PIC-MCC results is better at 2.45 GHz (figure 1(d)) than at 13.56 MHz (figure 2(d)). Analysis of the time-averaged power deposition profiles shown in figures 1(d) and 2(d) indicates that the ratio of power deposited in the sheaths to power deposited in the bulk decreases drastically as the driving frequency increases from 13.56 MHz to 2.45 GHz. This is a consequence of the variation of the electric field experienced by the electrons in the plasma. Current continuity requires the electric field in the sheath to be related to the field in the bulk region by a factor of  $\sim \omega_{\text{pe}}^2 / (\omega \cdot \nu)$  [15, 16]. Here  $\omega_{\text{pe}}$  is the electron plasma frequency,  $\omega$  is the driving frequency and  $\nu$  is the electron-neutral collision frequency. As a result, the power deposited in the bulk plasma increases with frequency and the

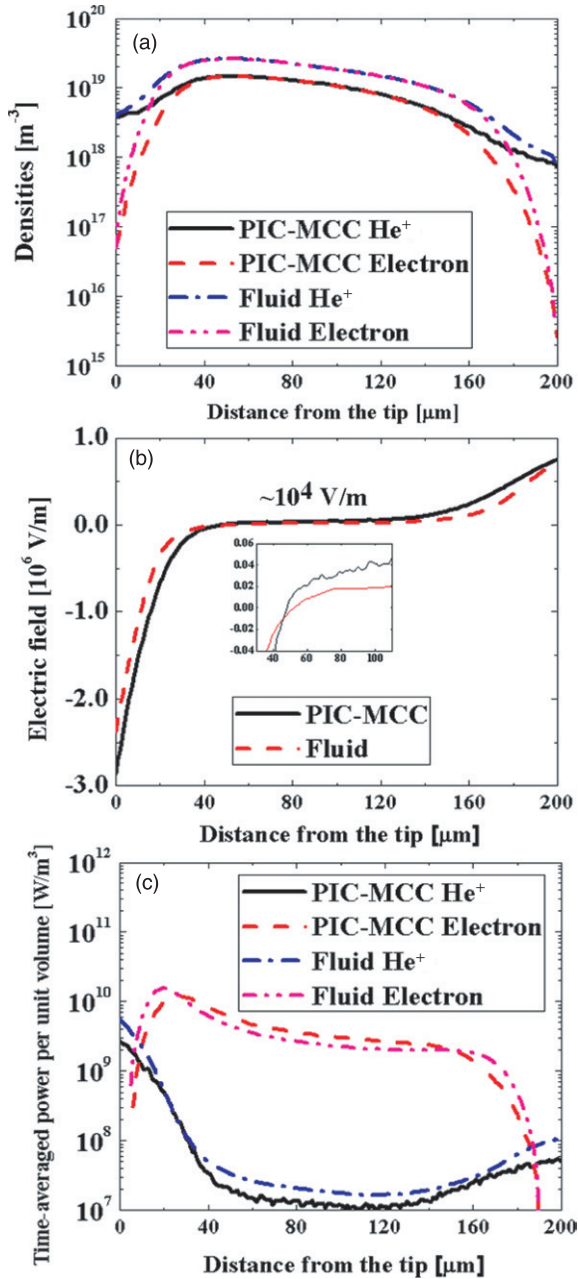


**Figure 1.** Comparison of PIC and fluid simulation results at 2.45 GHz of 15 A cm<sup>-2</sup>: (a) density, (b) electric field and (c) power deposition profiles. Two types of simulation models reproduced very similar results. In the plasma region, the density of fluid simulation is large by a factor of almost two times (a density of PIC simulation is about 10<sup>19</sup> m<sup>-3</sup> and one of fluid simulation is about 1.8 × 10<sup>19</sup> m<sup>-3</sup> at the position of 104 μm), and electric field obtained from PIC simulation was around 10<sup>4</sup> V m<sup>-1</sup>.

resulting power deposition profile gets flatter. This frequency effect is captured qualitatively in both models.

In order to understand the similarity or discrepancy between fluid and PIC-MCC simulation results, the electron kinetics should be analysed. Because the fluid model assumes the particle velocity/energy distribution function to be Maxwellian, the agreement between fluid and PIC-MCC simulation results depends on the validity of this assumption. PIC-MCC models provide the self-consistent electron energy

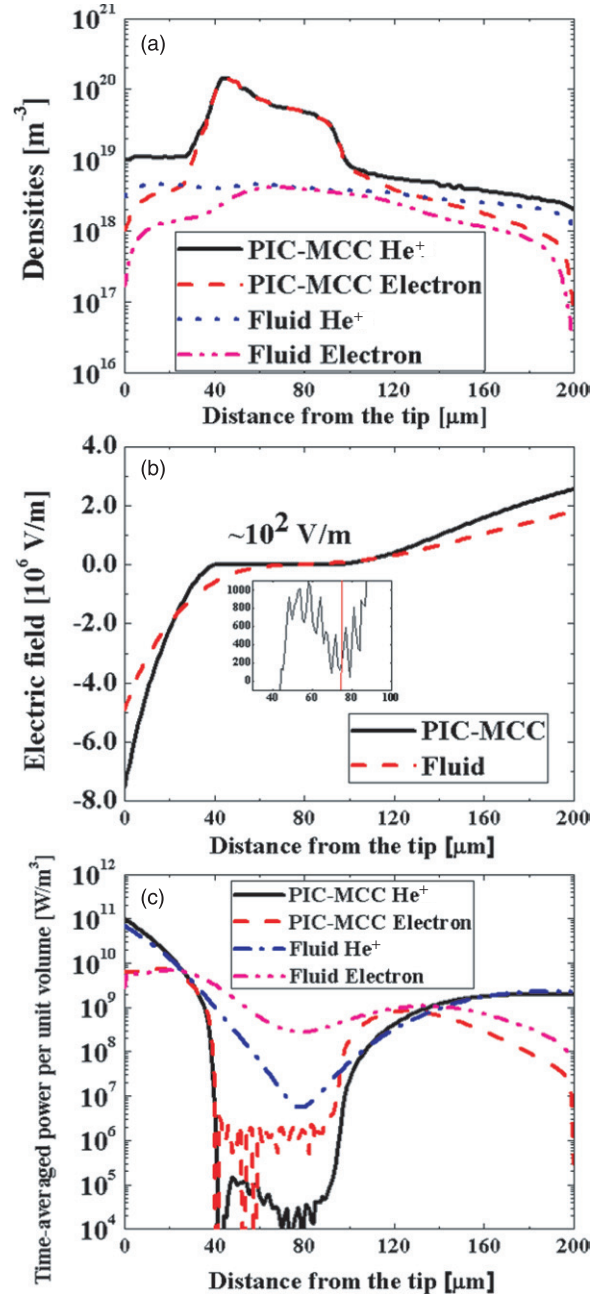


**Figure 2.** Comparison of PIC and fluid simulation results at 13.56 MHz of 1.6 A cm<sup>-2</sup>: (a) density, (b) electric field and (c) power deposition profiles. Both models gave different results especially at the plasma region. In the plasma region, the density of PIC simulation is large by a factor of almost ten times (a density of PIC simulation is about 5.1 × 10<sup>19</sup> m<sup>-3</sup> and one of fluid simulation is about 3.9 × 10<sup>18</sup> m<sup>-3</sup> at the position of 78 μm), and electric field obtained from PIC simulation was around 10<sup>2</sup> V m<sup>-1</sup>.

distribution function that develops in the plasma, a valuable tool to reveal the underlying physics governing these discharges. The electron energy probability functions (EEPFs) of the discharges driven by 13.56 MHz and 2.45 GHz are shown in figure 3. The EEPF is defined as  $f(\epsilon) = F(\epsilon) \cdot \epsilon^{-1/2}$ , where  $\epsilon$  is the electron energy and  $F(\epsilon)$  is the electron energy distribution function. Regardless of the magnitude or type of the driving source, and the measurement position within

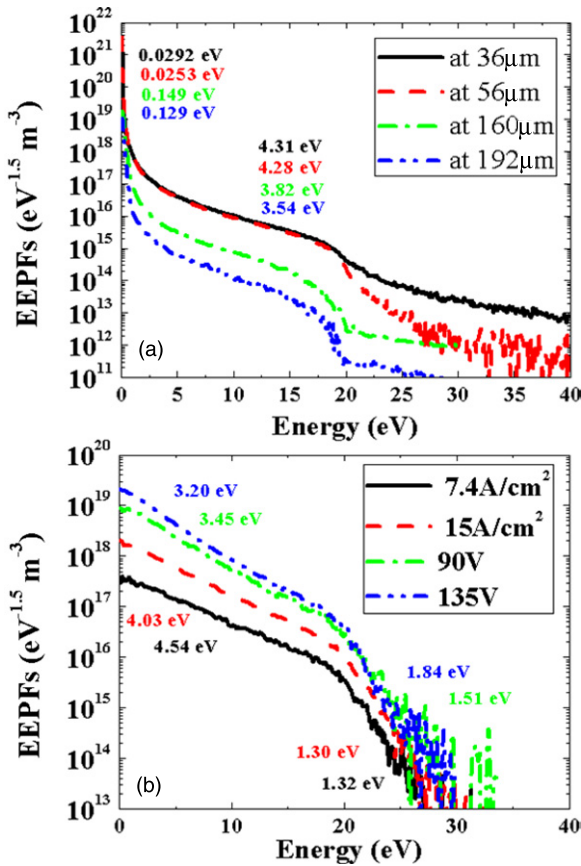


**Figure 3.** EEPFs (a) of the RF (13.56 MHz-1.6 A  $\text{cm}^{-2}$ ) discharge at several regions and (b) of the microwave (2.45 GHz) discharges at the peak density region. EEPFs in RF discharges show definitely the two-temperature shape but EEPFs in microwave discharges show just one temperature (close-to-Maxwellian); the electrons below 20 eV can be neglected because the electron population above 20 eV is much lower than the one below 20 eV.

the discharge, the EEPFs have a pronounced knee at around 20 eV (figure 3). This is due to the onset of inelastic collisions for electrons with energy above the excitation threshold of helium ( $\sim 20$  eV) [14]. As the driving frequency increases from 13.56 MHz to 2.45 GHz, the EEPF changes from a three-temperature distribution to a distribution that in the elastic regime closely resembles a Maxwellian distribution. A large number of low-energy electrons observed in the RF discharges (figure 3(a)) result from the trapping of low-energy electrons in the ambipolar potential and the inefficient heating of these electrons by the small RF field in the bulk plasma [14, 17]. As the frequency increases, on the other hand, the electric field experienced by the electrons in the bulk plasma also increases. This leads to an enhanced power deposition in the bulk plasma (figure 1(c)) and the evolution of the EEPF towards a Maxwellian distribution (figure 3). The large difference between the three-temperature EEPF obtained in the PIC-MCC simulations and the Maxwellian EEPF assumed in the fluid model leads to the large discrepancies observed in figure 2. As a result of the difference in the EEPF, the fluid model underestimates the number of low-energy electrons that are present in the bulk plasma. Assuming a two-temperature EEPF instead of a Maxwellian distribution could lead to fluid models

with enhanced fidelity suitable for the study of atmospheric pressure RF discharges.

#### 4. Conclusion

This study has presented a comparison of fluid and PIC-MCC simulations of helium microdischarges at atmospheric pressure. Both simulation techniques predict qualitatively similar plasma density, electric field and power deposition profiles. The degree of agreement between fluid and PIC-MCC simulations, however, varies with the driving frequency. It is shown that changes in the driving frequency cause changes in the electron energy distribution function, and as a result the validity of the assumption of a Maxwellian electron distribution that is made in the fluid model varies.

PIC-MCC simulations provide the evolution of the electron energy distribution function as the driving frequency increases from 13.56 MHz to 2.45 GHz. The enhanced electron heating in the bulk plasma at high frequency causes the three-temperature EEPF observed in RF discharges to evolve to a close-to-Maxwellian distribution. Since the reliability of fluid models depends on the validity of the assumption made with regard to the electron energy distribution function [9, 18, 19], the closer the electron energy distribution function is to the assumption made in the fluid model the closer the simulation results are. As a result the simulation results of fluid and PIC-MCC models agree reasonably well at 2.45 GHz. It is suggested that developing a fluid model in which the electron energy distribution function is assumed to be similar to that obtained in the PIC-MCC simulations would result in an improved tool for fast analysis of RF microdischarges.

#### Acknowledgments

This work was supported in part by the Korea Science and Engineering Foundation (KOSEF) grant funded by the Korea government (MOST) (No R01-2007-000-10730-0) and the Korea Ministry of Education through its Brain Korea 21 program.

#### References

- [1] Laroussi M, Tendero C, Lu X, Alla S and Hynes W L 2006 *Plasma Process. Polym.* **3** 470
- [2] Stoffels E, Kieft I E and Sladek R E J 2003 *J. Phys. D: Appl. Phys.* **36** 2908–13
- [3] Deng X T, Shi J J and Kong M G 2007 *J. Appl. Phys.* **101** 074701
- [4] Godyak V A, Piejak R B and Alexandrovich B M 1992 *Phys. Rev. Lett.* **68** 40
- [5] Tachibana K, Mizokami K, Kosugi N and Sakai T 2003 *IEEE Trans. Plasma Sci.* **31** 68
- [6] Wang Q, Koleva I, Donnelly V M and Economou D J 2005 *J. Phys. D: Appl. Phys.* **38** 1690
- [7] Donkó Z, Hartmann P and Kutasi K 2006 *Plasma Sources Sci. Technol.* **15** 178
- [8] Wang Q, Economou D J and Donnelly V M 2006 *J. Appl. Phys.* **100** 023301
- [9] Kim H C, Iza F, Yang S S, Radmilovic-Radjenovic M and Lee J K 2005 *J. Phys. D: Appl. Phys.* **38** R283–301

- [10] Choi J, Iza F, Lee J K and Ryu C M 2007 *IEEE Trans. Plasma Sci.* **35** 1274–8
- [11] Wichaidit C and Hitchon W N G 2005 *J. Comput. Phys.* **203** 650–67
- [12] Birdsall C K and Langdon A B 1985 *Plasma Physics via Computer Simulation* (New York: McGraw-Hill)
- [13] Verboncoeur J P 2005 *Plasma Phys. Control. Fusion* **47** A231
- [14] Hong Y J, Lee S M, Kim G C and Lee J K 2008 *Plasma Process. Polym.* **5** 583–92
- [15] Lieberman M A and Lichtenberg A J 2005 *Principles of Plasma Discharges and Materials Processing* 2nd edn (New York: Wiley)
- [16] Iza F, Kim G J, Lee S M, Lee J K, Walsh J L, Zhang Y T and Kong M G 2008 *Plasma Process. Polym.* **5** 322
- [17] Iza F, Lee J K and Kong M G 2007 *Phys. Rev. Lett.* **99** 075004
- [18] Gudmundsson J T 2001 *Plasma Sources Sci. Technol.* **10** 76–81
- [19] Nam S K and Verboncoeur J P 2008 *Appl. Phys. Lett.* **92** 231502